REPORT DOCUMENTATION PAGE

Form Approved
OMB No. 0704-0188

1. REPORT DATE *(DD-MM-YYYY)*	**2. REPORT TYPE**	**3. DATES COVERED** *(From - To)*
27 July 2016	Briefing Charts	21 July 2016 – 31 August 2016

4. TITLE AND SUBTITLE
Modeling of Fuel Film Cooling Using Steady State RANS and Unsteady DES Approaches

5a. CONTRACT NUMBER

5b. GRANT NUMBER

5c. PROGRAM ELEMENT NUMBER

6. AUTHOR(S)
Kevin C. Brown, Edward B. Coy, Matthew E. Harvazinski, Venkateswaran Sankaran

5d. PROJECT NUMBER

5e. TASK NUMBER

5f. WORK UNIT NUMBER
Q0VZ

7. PERFORMING ORGANIZATION NAME(S) AND ADDRESS(ES)

Air Force Research Laboratory (AFMC)
AFRL/RQRC
10 E. Saturn
Edwards AFB, CA 93524-7680

8. PERFORMING ORGANIZATION REPORT NO.

9. SPONSORING / MONITORING AGENCY NAME(S) AND ADDRESS(ES)

Air Force Research Laboratory (AFMC)
AFRL/RQR
5 Pollux Drive
Edwards AFB, CA 93524-7048

10. SPONSOR/MONITOR'S ACRONYM(S)

11. SPONSOR/MONITOR'S REPORT NUMBER(S)
AFRL-RQ-ED-VG-2016-248

12. DISTRIBUTION / AVAILABILITY STATEMENT
Approved for Public Release; Distribution Unlimited.

13. SUPPLEMENTARY NOTES
For presentation at AIAA Propulsion and Energy 2016; Salt Lake City, Utah (27 July 2016)
PA Case Number: #16391; Clearance Date: 8/16/2016

14. ABSTRACT
Viewgraph/Briefing Charts

15. SUBJECT TERMS
N/A

16. SECURITY CLASSIFICATION OF:			**17. LIMITATION OF ABSTRACT**	**18. NUMBER OF PAGES**	**19a. NAME OF RESPONSIBLE PERSON**
a. REPORT	**b. ABSTRACT**	**c. THIS PAGE**			E. Coy
Unclassified	**Unclassified**	**Unclassified**	SAR	30	**19b. TELEPHONE NO** *(include area code)* N/A

Standard Form 298 (Rev. 8-98)
Prescribed by ANSI Std. 239.18

Modeling of Fuel Film Cooling Using Steady State RANS and Unsteady DES Approaches

Kevin Brown, Air Force Research Laboratory

AIAA Propulsion and Energy 2016

27 July, 2016

Overview

- Introduction
- Numerical Approach
- Baseline and Parametric Cases
- Results
- Conclusions and Future Work

Introduction

- **Fuel film cooling is critical for high performing boost engines using the Oxygen Rich Staged Combustion Cycle**
  - Reduces heat load and closes the power balance
  - Reduces the required coolant channel pressure drop
  - Must be efficient or I_{sp} will be affected
  - Film cooling schemes are not optimized

Introduction

- **FFC inlets can have complex instabilities**
  - Acoustic resonance modes
  - Kelvin-Helmholtz instabilities
  - Shear layer impingement
- **Difficult to capture computationally**
  - High density gradients
  - Complex chemistry
  - Trans- and supercritical fluid behavior
  - Thermal radiation, soot formation, etc.

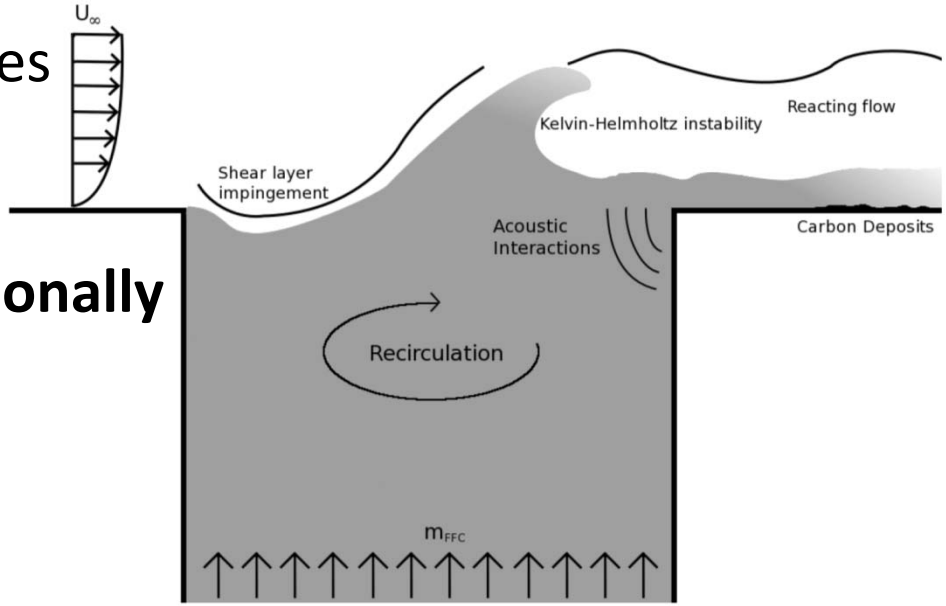

Previous work

- **Comparison with experiments in a subscale fuel film cooled thrust chamber**
  - 2D steady state RANS with ideal gas and equilibrium chemistry (Himansu et al. 2014)
  - Over-predicted film cooling effectiveness near FFC inlet
  - Under-predicted performance further downstream
  - Does not capture trends in changing mass flow rate

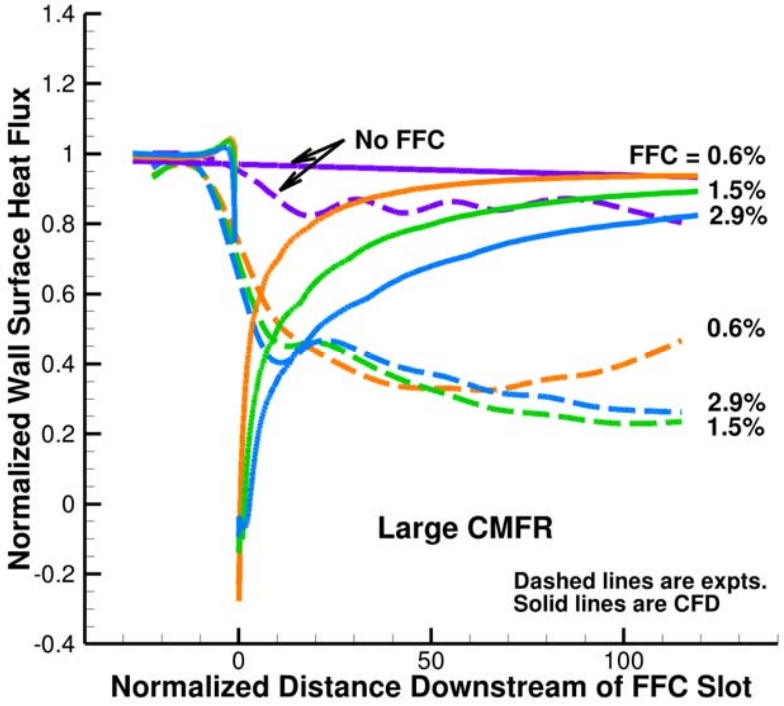

Hypothesis: Unsteady, pulsing, flow results in a measured heat flux that is the average of an uncooled and an overcooled wall. Steady RANS cannot capture this effect.

Current Objectives

- **Capture unsteady flow effects in FFC simulations**
  - Determine most relevant physics to thermal management simulations
  - Incorporate complex physics into simulation suite
  - Reproduce results seen experimentally in wall heat flux
- **Determine if added cost of unsteady simulations improves predictive capabilities**

Numerical Methods

- **Using General Equation and Mesh Solver (GEMS)**
  - Unstructured mesh solver
  - Second-order accurate in time and space
- **Ideal gas law used for initial study**
  - More stable calculations, but not all fluid properties are represented accurately.
  - Density ratios controlled by modifying molecular weight

Numerical Methods

- **Unsteady time-accurate simulations**
  - Detached eddy simulations (DES)
    - LES subgrid models used in region where grid is fine
    - Improved performance over RANS without cost of full LES
    - Turbulence computed using the k-ω model
- **Steady state simulations**
  - Reynolds-Averaged Navier-Stokes (RANS)
  - Used as initial condition for unsteady simulations

Baseline and Parametric Cases

- **All 2D, same baseline geometry as Himansu et al.**
- **No conjugate heat transfer**
  - Adiabatic wall temperature calculations in place of wall heat flux

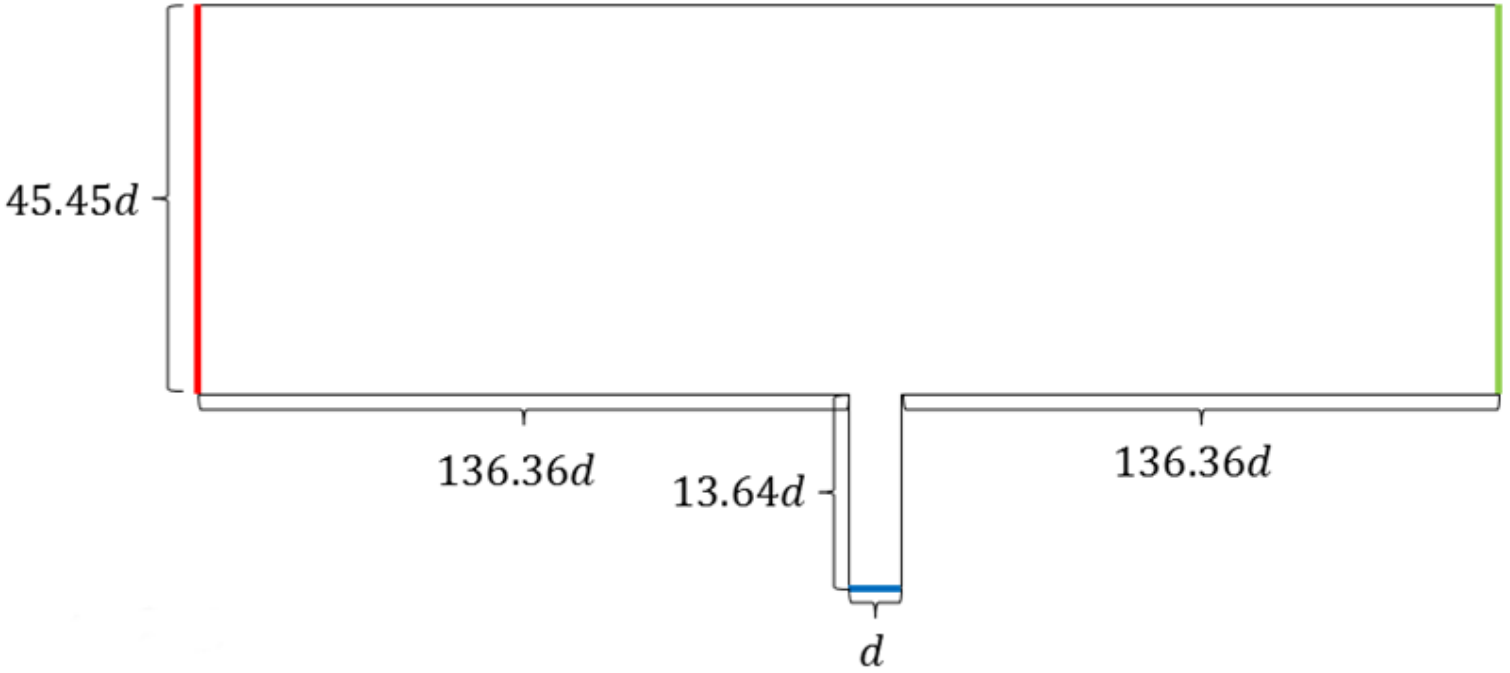

Parametric Studies

- **Baseline case chosen from in-house experimental setup**
- **Parametric studies will vary around this set of conditions**
- **Results can be compared to experimental trends**

Table 1. Flow conditions for baseline case

Pressure (MPa)	5.2	Slot Width (m)	5.6×10^{-4}
FFC Temperature (K)	350	Main chamber temperature	3680
FFC mass flow rate (kg/s)	0.41	Main chamber mass flow rate	25.64
FFC velocity (m/s)	1.1	Main chamber velocity	237.5
FFC density (kg/m^3)	638	Main Chamber density	4.4
FFC Reynolds number	3.8×10^4	Main chamber Reynolds number	2.4×10^5
Mass flow ratio	1.6×10^{-2}	Mach number	0.2
Momentum ratio	7.9×10^{-5}	Density Ratio	145

Parametric Studies

- **First study: Vary main chamber mass flow rate, FFC mass flow rate to produce range of mass flow ratios at constant fuel density**
  - Initial study to determine if unsteadiness is significant
- **Second study: Vary density of fuel film, hold momentum ratio and mass flow ratio constant**
  - Determine if observed frequencies depend on fuel density
- **Third Study: Vary slot width, hold mass flow ratio, momentum ratio, and density constant**
  - Determine if velocity trends can be collapsed

Parametric Studies

Parametric study	Constant density and slot width, varying mass flow rates and momentum	Constant mass flow rates and momentum, varying density and slot width	Constant density, varying slot width and momentum
Reynolds number	$\approx 10^5 - 10^6$	$\approx 10^5$	$\approx 10^5$
Slot width (m)	5.6×10^{-4}	$3.8 - 11 \times 10^{-4}$	$3.8 - 11 \times 10^{-4}$
Main chamber density (kg / m^3)	$4.31 - 4.44$	4.42	4.42
Main chamber velocity (m/s)	$50 - 273$	233	233
Fuel density (kg / m^3)	638	$146 - 432$	295
Fuel velocity (m/s)	$0.7 - 5.4$	$1.2 - 1.6$	$1 - 3$
Momentum thickness (m)	$1.5 - 2.4 \times 10^{-4}$	1.6×10^{-4}	1.6×10^{-4}
Mass flow ratio	$0.01 - 0.075$	0.014	0.014
Density ratio	145	$33 - 97$	67
Momentum ratio	$10^{-4} - 10^{-3}$	$\approx 10^{-4}$	$\approx 10^{-4}$
Mach number	0.05-0.33	0.2	0.2

Quantities Varied in Parametric Study

Parametric Studies

Parametric Study	#1	#2	#3
Reynolds number	$O(10^5 - 10^6)$	$O(10^5)$	$O(10^5)$
Slot width (m)	5.6×10^{-4}	$3.8 - 11 \times 10^{-4}$	$3.8 - 11 \times 10^{-4}$
Main chamber density (kg/m^3)	4.4	4.4	4.4
Main chamber velocity (m/s)	50—273	233	233
Fuel density (kg/m^3)	638	146—432	295
Fuel velocity (m/s)	0.7—5.4	≈ 1.4	1—3
Mass flow ratio (kg/s)	0.01—0.075	0.014	0.014
Density ratio	145	33—97	67
Momentum ratio	$O(10^{-4} - 10^{-3})$	$O(10^{-4})$	$O(10^{-4})$
Mach number	0.05—0.32	0.20	0.20

Quantities Varied in Parametric Study

Unsteady DES

- **Baseline case**

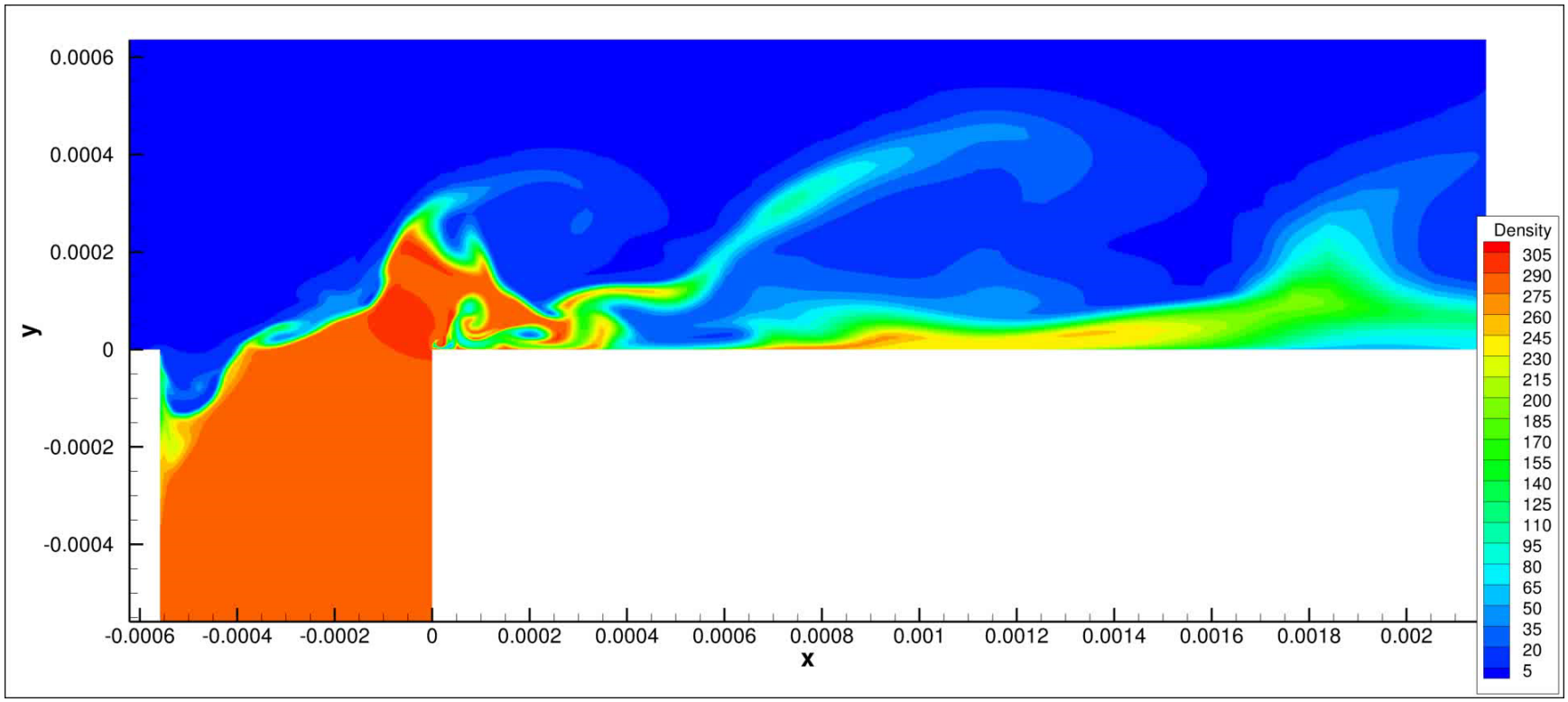

Comparison of RANS and DES

- **Baseline case**

Fuel mass fraction

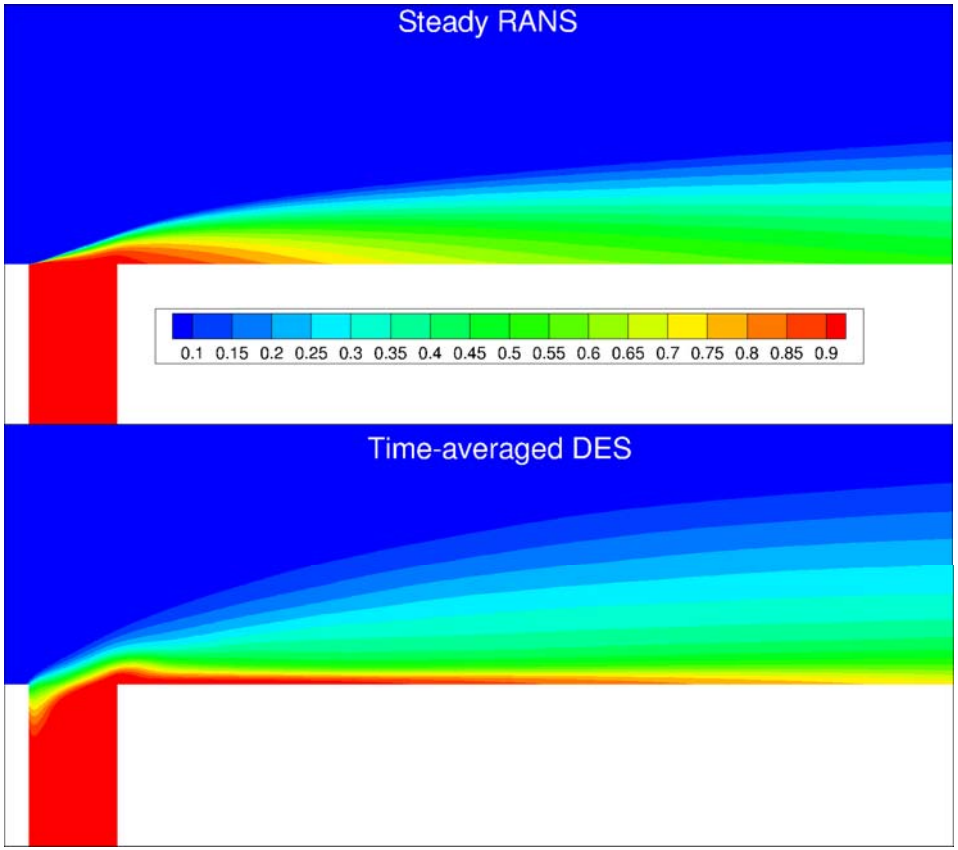

Temperature

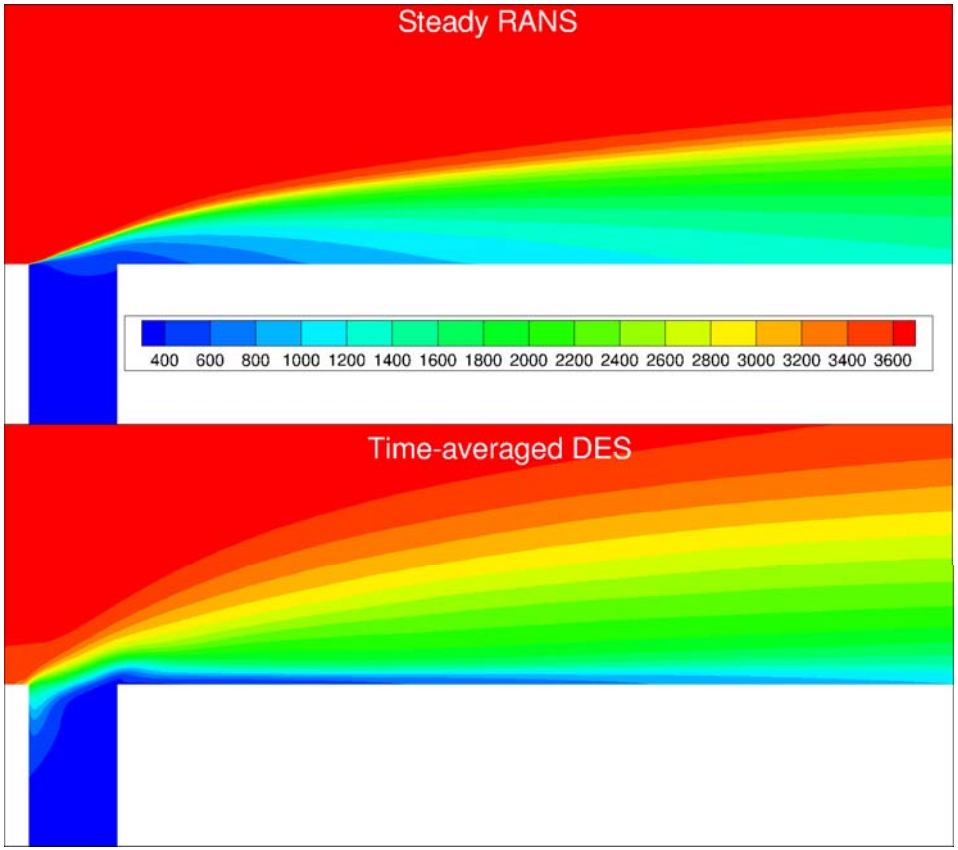

Adiabatic Wall Temperatures

- **Adiabatic wall temperature profiles**

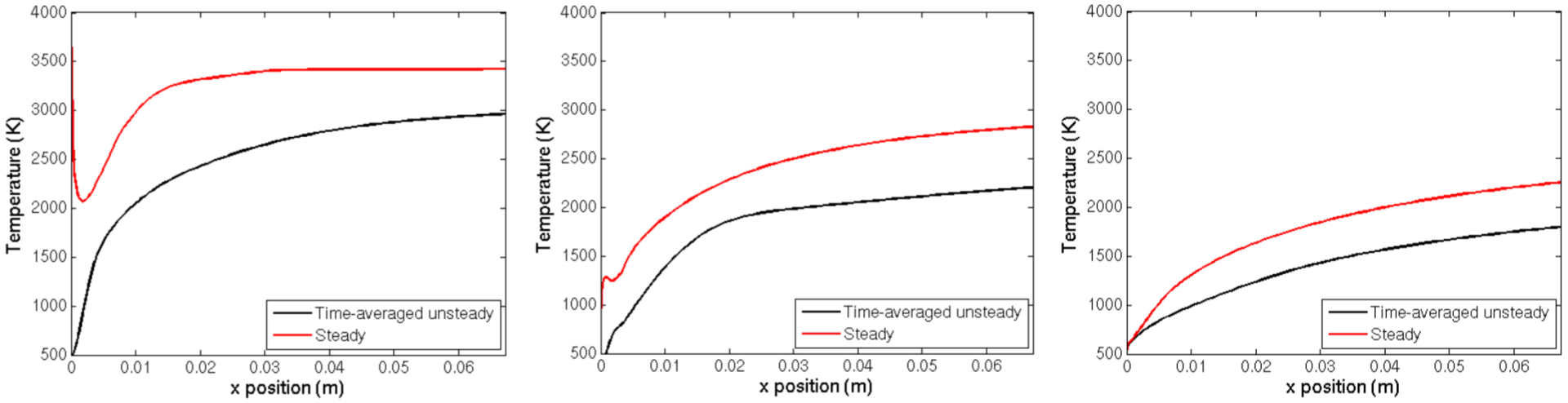

Increasing mass flow ratio

Adiabatic Effectiveness

- **Non-dimensionalize as adiabatic effectiveness:**

$$\eta = \frac{T_f - T_{aw}}{T_f - T_{FFC}}$$

T_f = freestream flow temperature

T_{aw} = adiabatic wall temperature

T_{FFC} = fuel film injection temperature

- **Allows for easy comparison of all three parametric studies**
- **Compare to experimental trends for qualitative analysis**

Adiabatic Effectiveness

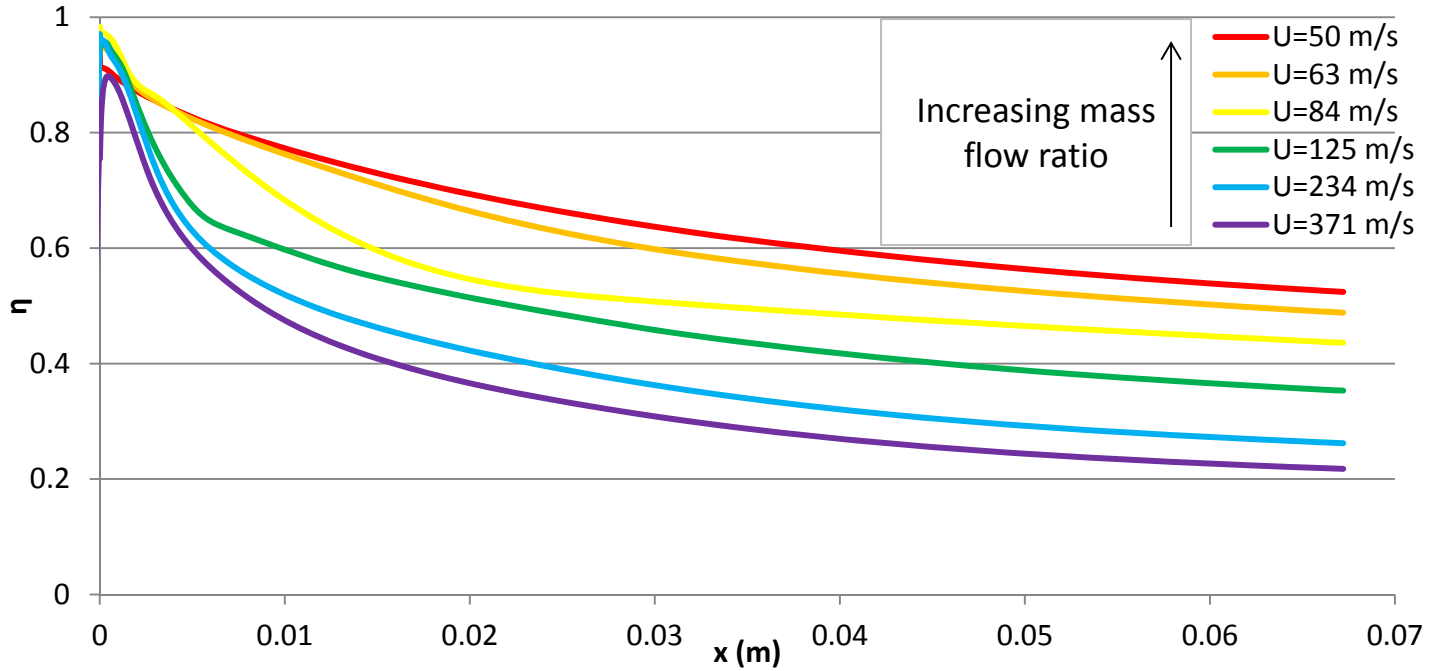

Mass flow varies, constant density/slot width					
FFC Velocity (m/s)	1.15	Main Velocity	50—371	Main Mach	0.05—0.32
FFC Density (kg/m^3)	638.51	Main Density	4.41	Density Ratio	145
FFC slot width (m)	5.6×10^{-4}	Mass flow ratio	1.0×10^{-2} – 7.5×10^{-2}	Momentum ratio	3.1×10^{-5} – 1.7×10^{-3}

Adiabatic Effectiveness

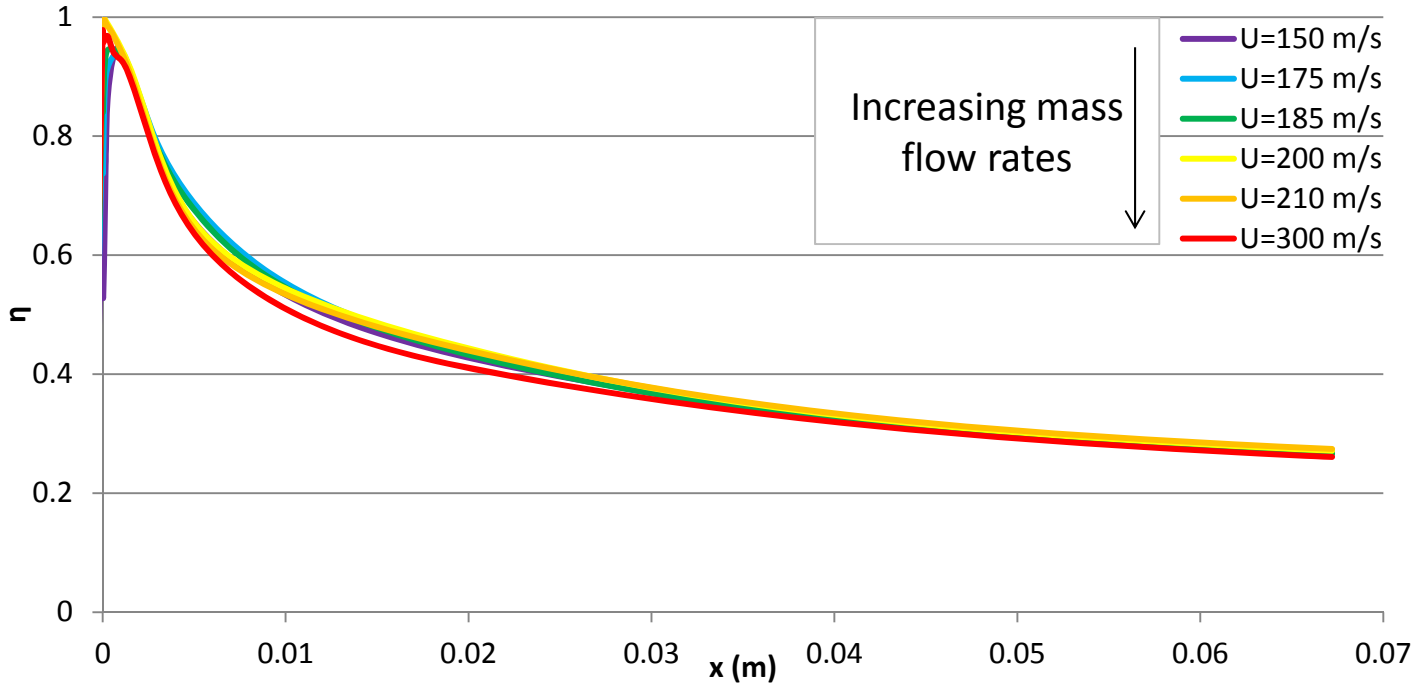

Both mass flow rates vary, constant density/slot width/mass flow ratio					
FFC Velocity (m/s)	0.7—1.4	Main Velocity	150—300	Main Mach	0.13—0.26
FFC Density (kg/m^3)	640	Main Density	4.4	Density Ratio	145
FFC slot width (m)	5.6×10^{-4}	Mass flow ratio	1.6×10^{-2}	Momentum ratio	7.9×10^{-5}

Adiabatic Effectiveness

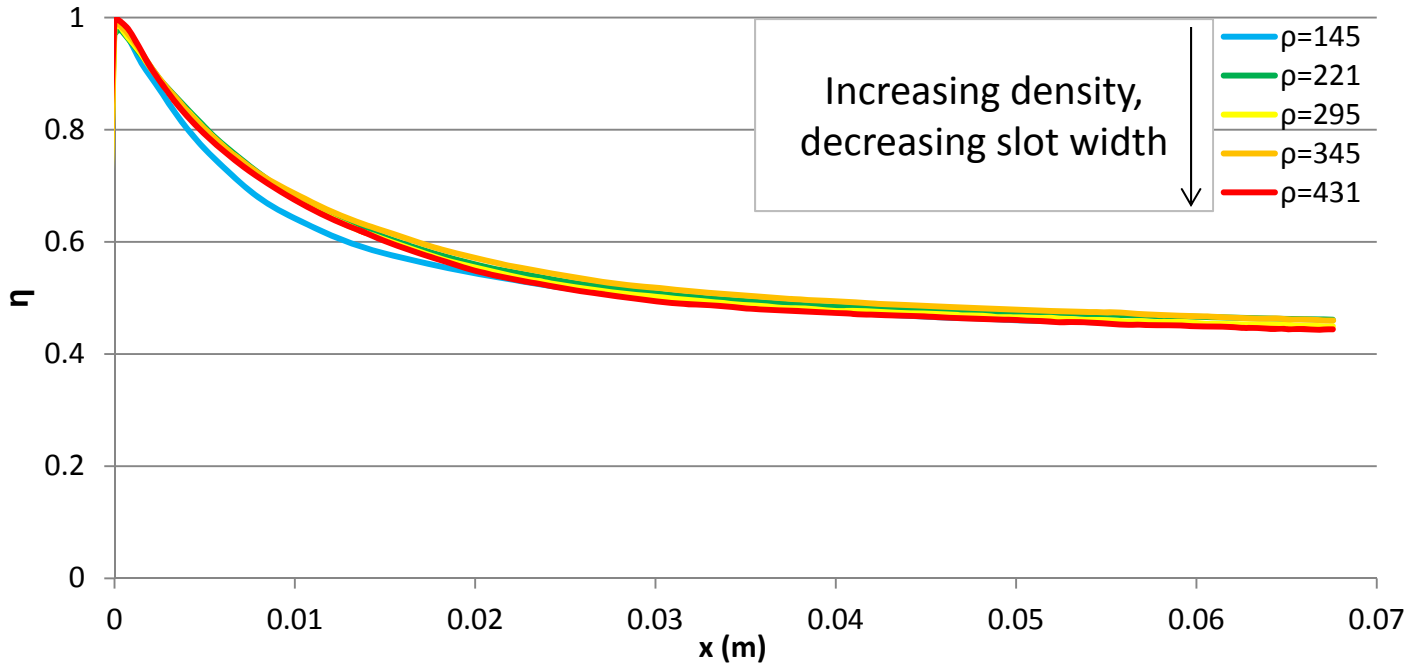

Density varies, slot width varies, constant mass flow/momentum					
FFC Velocity (m/s)	2.12	Main Velocity	233.4	Main Mach	0.2
FFC Density (kg/m^3)	145—430	Main Density	4.411	Density Ratio	33—98
FFC slot width (m)	3.8×10^{-4} – 1.1×10^{-3}	Mass flow ratio	1.4×10^{-2}	Momentum ratio	1.2×10^{-4}

Adiabatic Effectiveness

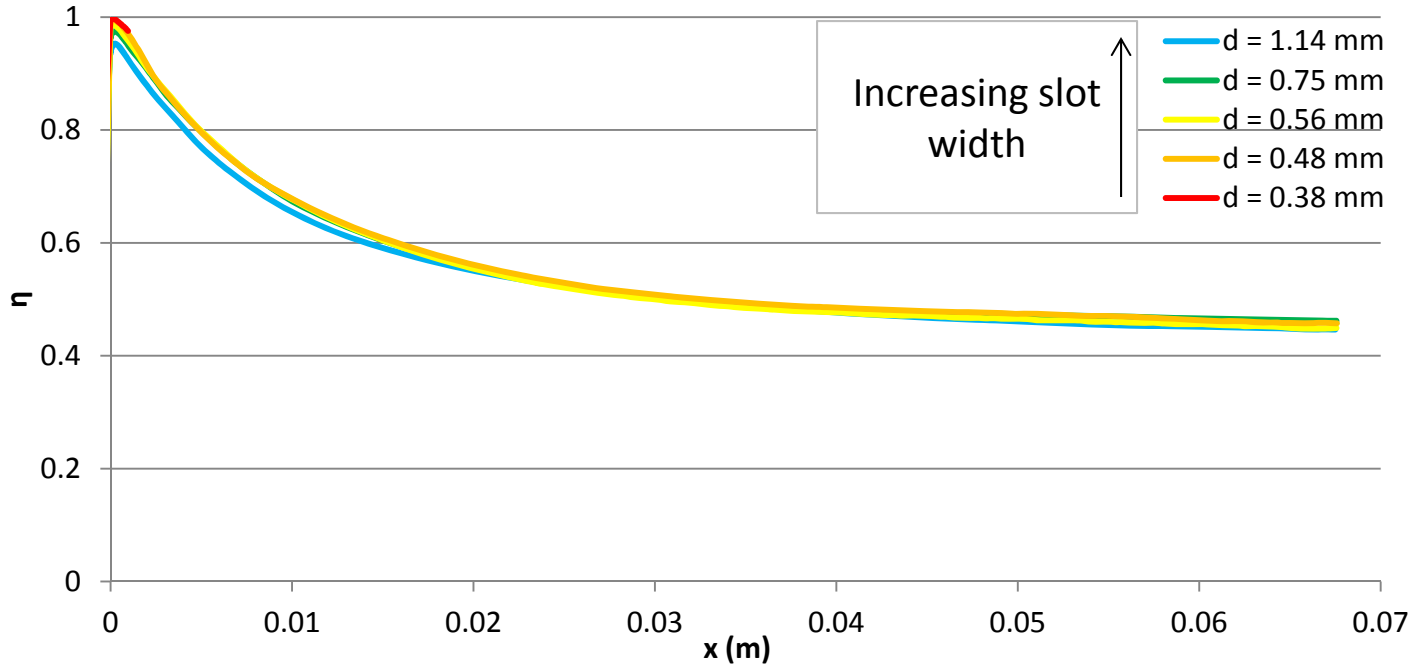

Slot width varies, constant density/mass flow					
FFC Velocity (m/s)	1—3	Main Velocity	233	Main Mach	0.2
FFC Density (kg/m^3)	295	Main Density	4.4	Density Ratio	67
FFC slot width (m)	$3.8 \times 10^{-4} - 1.1 \times 10^{-3}$	Mass flow ratio	1.4×10^{-2}	Momentum ratio	$6.1 \times 10^{-5} - 1.8 \times 10^{-4}$

Steady v. Unsteady Effectiveness

- Main mass flow rate changes, density and slot width constant

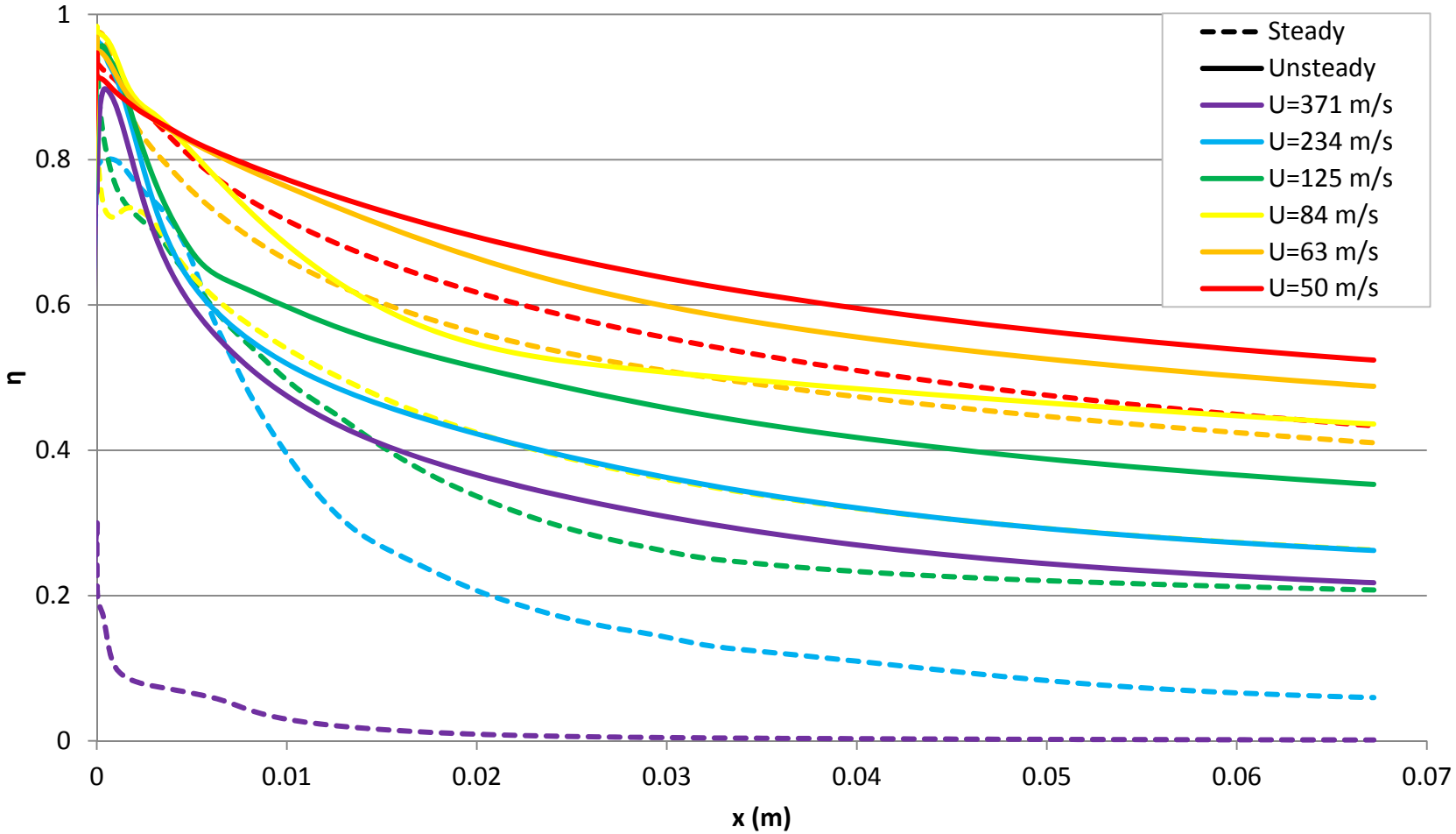

Adiabatic Effectiveness

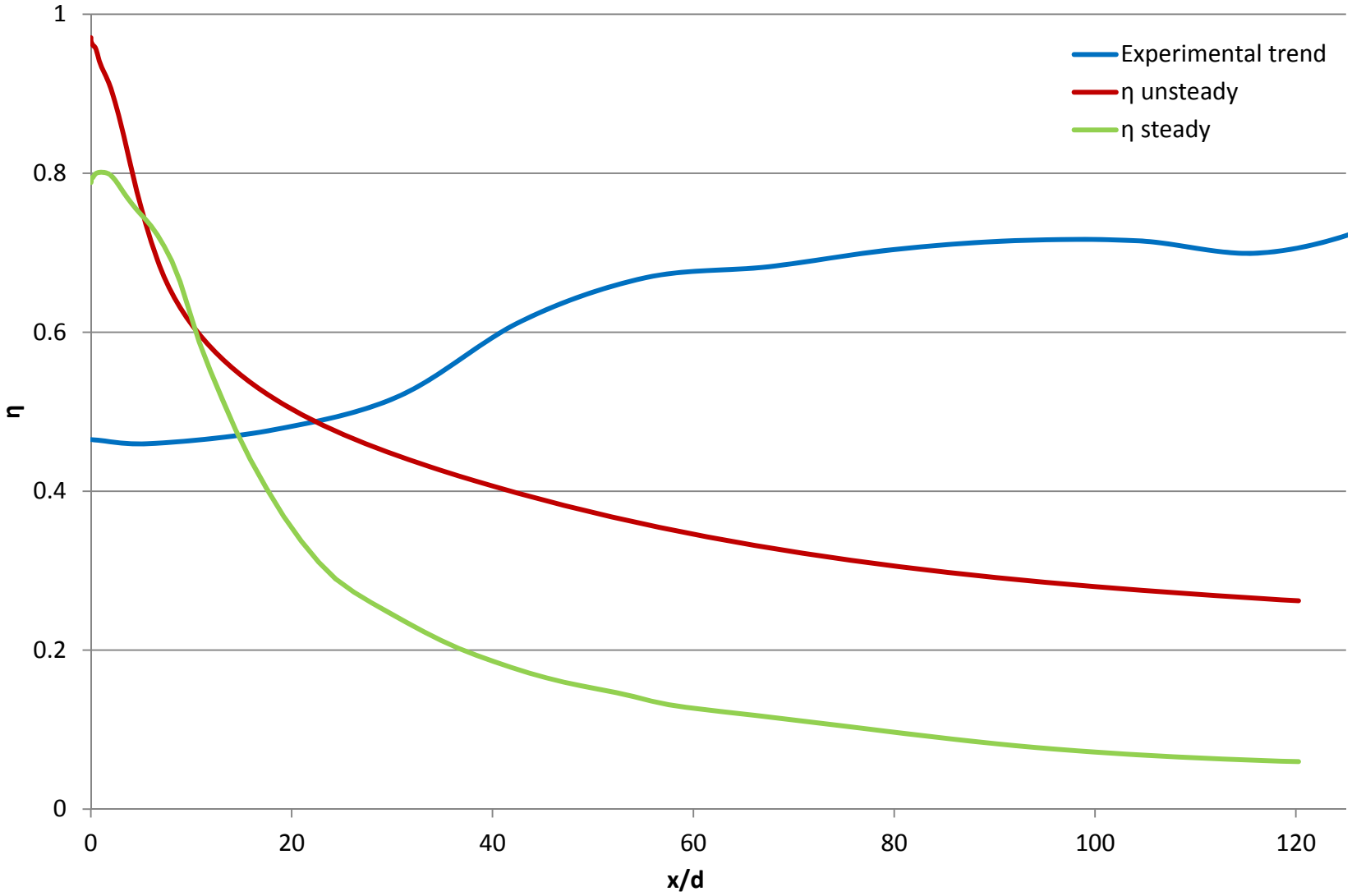

Power Spectral Density

- **Baseline case**

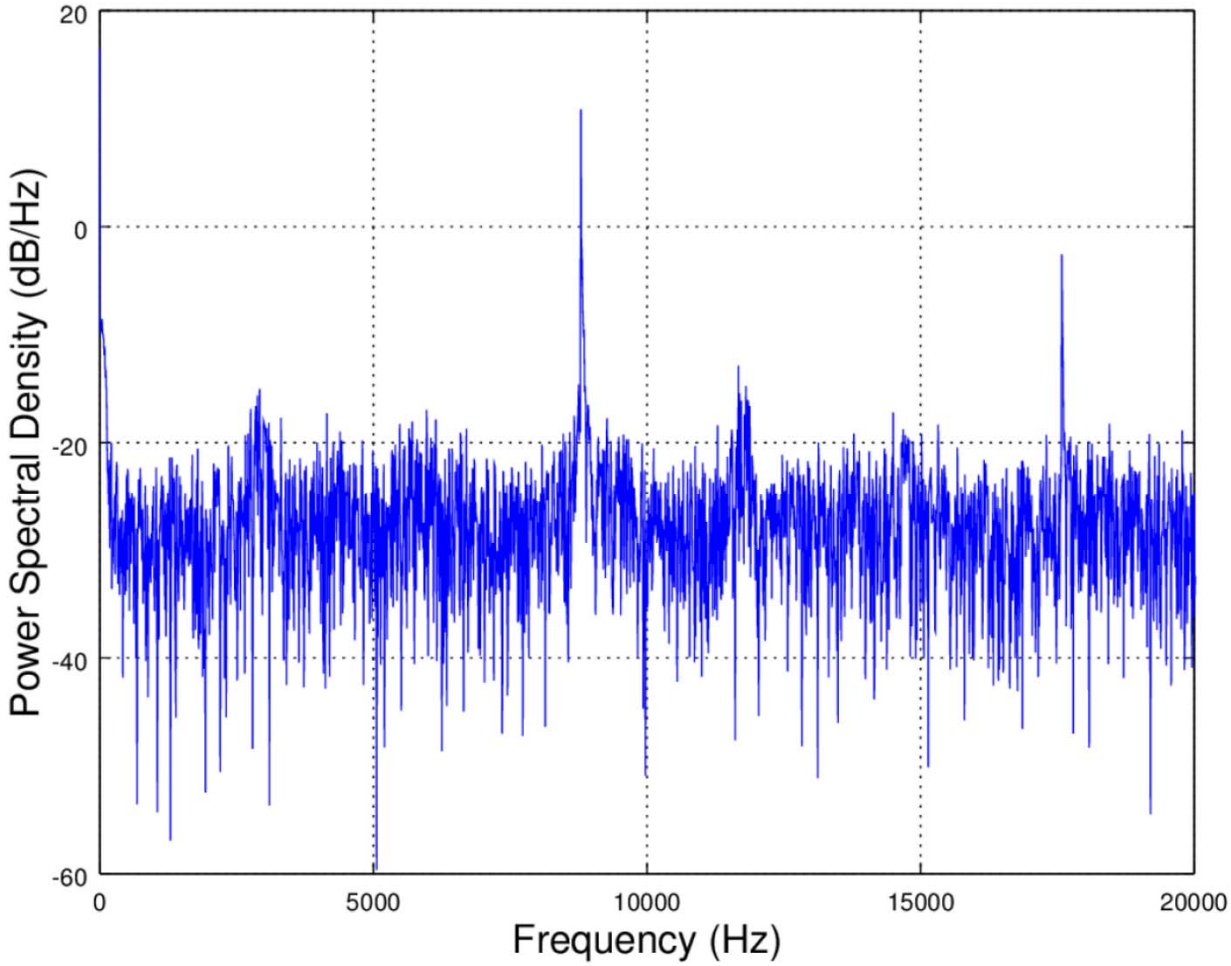

Power Spectral Density

- **First parametric study**
  - Increasing main chamber mass flow, FFC mass flow rate held constant

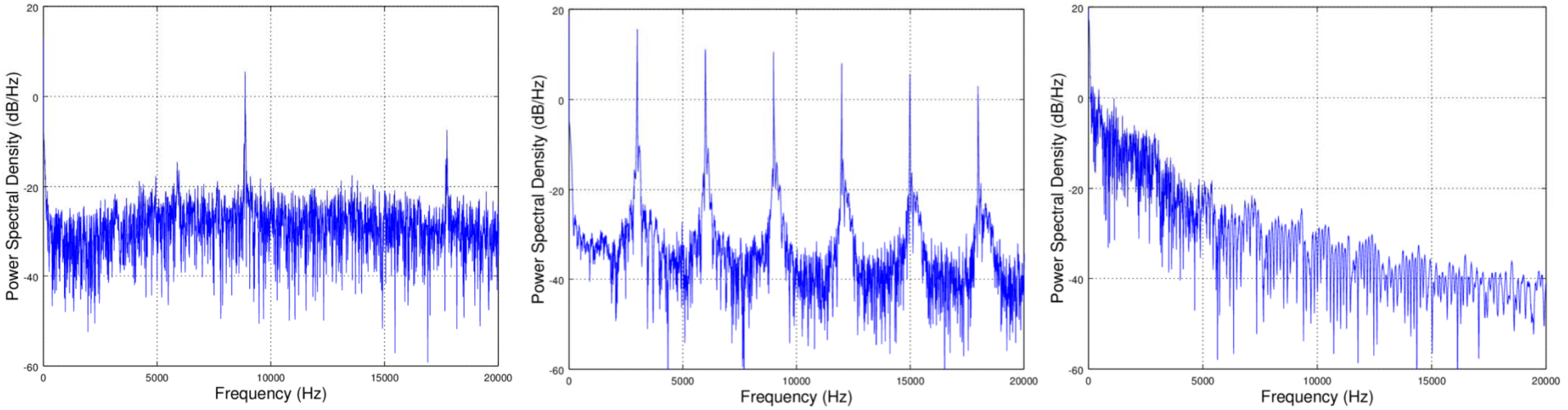

Increasing mass flow ratio

Nondimensionalization

- **Frequency of fuel film oscillations is not constant**
  - Seems to switch between two modes
- **Helmholtz number for each case:**

$$\mathrm{He} = \frac{2\pi f}{cd}$$

f =frequency

c = speed of sound (m/s)

d = depth of FFC inlet

  - Integer values mean inlet is functioning as resonator
  - Calculated He for three most dominant frequencies in each case

Helmholtz number v. Mach number

- **Resonant frequencies for first parametric study**

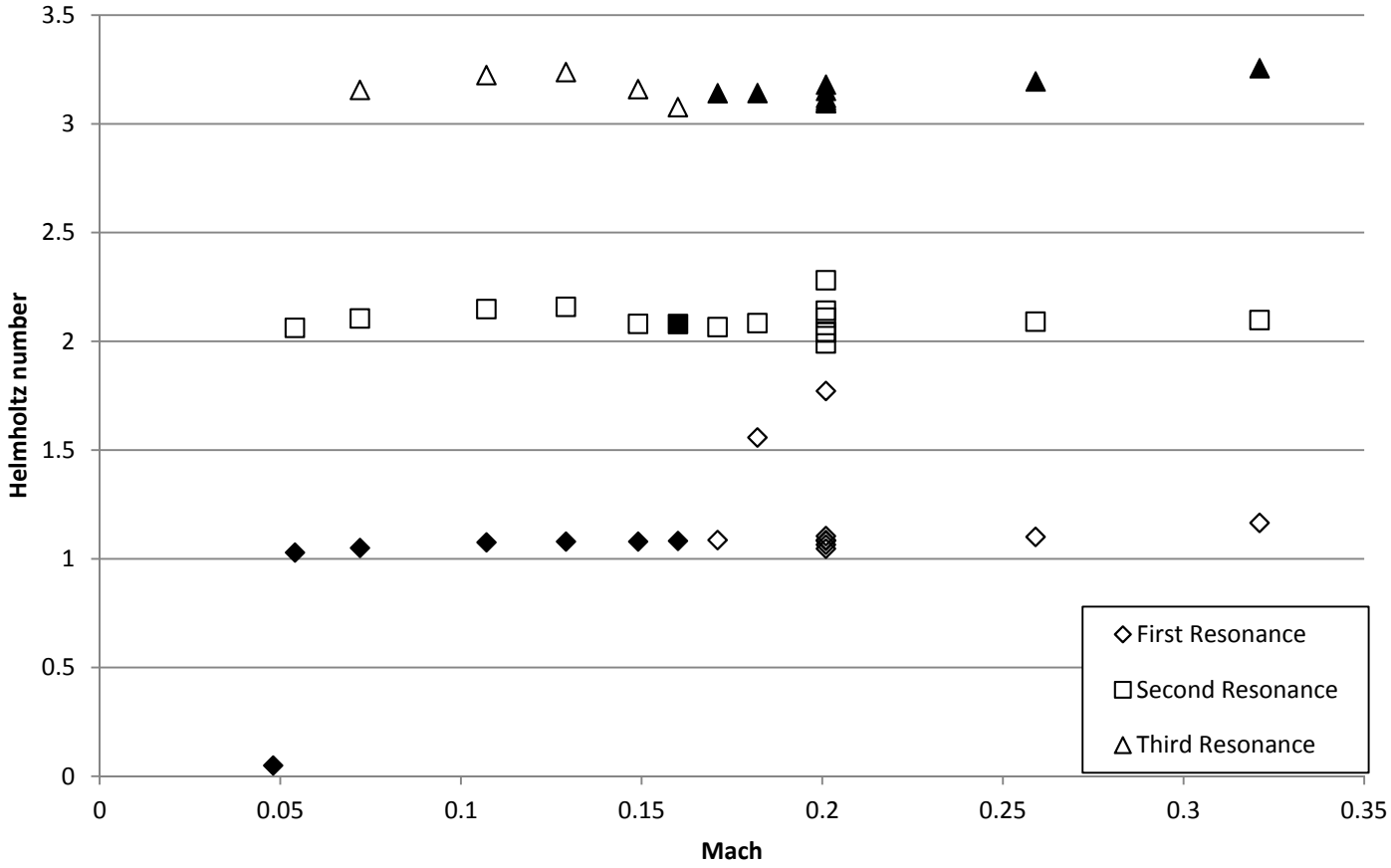

Conclusions

- **Significant differences between steady, unsteady simulations**
  - Capture of additional flow features justifies the increased computational cost of unsteady simulations
  - Unsteady simulations predict lower average heat flux past x/d=15, consistent with original hypothesis
- **Mass flow ratio is primary driver of adiabatic effectiveness**
  - Density ratio is also a factor
- **Unsteadiness in these cases driven by Helmholtz mode of inlet slot**
  - Inlet geometry important for film cooling effectiveness
- **Still significant discrepancies between CFD and experimental results**
  - May be due to soot deposition, radiative heat transfer, or other complex physical phenomena

Future Work

- **Three-dimensional simulations**
  - Transverse waves may affect wall temperature profile
  - May also model more realistic FFC inlets
- **Real Gas Equation of State**
  - Capture supercritical properties
- **Introduce additional physics**
  - Soot formation and deposition
  - Radiative heat transfer